X-ray Structural Analyses of Symmetrically and Unsymmetrically Substituted μ_3-η^3-C_3R_3 Complexes of Ruthenium: $(\mu$-H)$Ru_3(\mu_3$-η^3-CMeCMeCMe)$(CO)_9$, $(\mu$-H)$Ru_3(\mu_3$-η^3-CMeCMeCOMe)$(CO)_9$, and $(\mu$-H)$Ru_3(\mu_3$-η^3-CMeCMeCSEt)$(CO)_9$.[1-5] Influence of π-Donor Substituents upon Nido–Arachno Polyhedral Distortion

Melvyn Rowen Churchill,* Lisa A. Buttrey, and Jerome B. Keister*

Department of Chemistry, University at Buffalo, State University of New York, Buffalo, New York 14214

Joseph W. Ziller

Department of Chemistry, University of California, Irvine, California 92717

Thomas S. Janik and William S. Striejewske

Department of Chemistry, College at Fredonia, State University of New York, Fredonia, New York 14063

Received September 1, 1989

Single-crystal X-ray diffraction studies of the title commpounds have been performed. Comparison of these structures with that of $(\mu$-H)$Ru_3(\mu_3$-η^3-CMeCHCNEt$_2)(CO)_9$, previously reported, provide evidence that π-donor substituents on the C_3 unit cause distortion of the Ru_3C_3 polyhedron from a nido toward an arachno structure, based upon a pentagonal-bipyramidal skeleton. The μ_3-η^3-CMeCMeCMe complex crystallizes in space group *Pnma* (No. 62) with a = 17.483 (11) Å, b = 16.033 (9) Å, c = 7.105 (3) Å, V = 1992 (2) Å^3, and Z = 4. The structure was refined to R_F = 3.9% for 1348 data (Mo Kα, 2θ = 4.0–45.0°, $|F_o| > 0$) and R_F = 2.7% for 1111 data with $|F_o| > 6\sigma(|F_o|)$. The μ_3-η^3-CMeCMeCOMe complex crystallizes in space group $P2_1/n$ (No. 14) with a = 9.581 (2) Å, b = 20.470 (3) Å, c = 10.7003 (15) Å, β = 106.400 (13)°, V = 2013.5 (5) Å^3, and Z = 4; refinement converged with R_F = 3.5% for 3356 data (2θ = 4.5–50.0°, $|F_o| > 0$) and R_F = 2.4% for 2739 data with $|F_o| > 6\sigma(|F_o|)$. The μ_3-η^3-CMeCMeCSEt complex crystallizes in space group $P2_1/n$ (No. 14) with a = 10.0275 (13) Å, b = 16.430 (3) Å, c = 13.812 (2) Å, β = 107.976 (11)°, V = 2164.4 (6) Å^3, and Z = 4; refinement converged with R_F = 5.1% for 2736 data (2θ = 4.0–45.0°, $|F_o| > 0$) and R_F = 4.2% for those 2308 data with $|F_o| > 6\sigma(|F_o|)$. The three complexes each contain two Ru(CO)$_3$ groups bridged by a hydride ligand and linked to a further Ru(CO)$_3$ group; the μ_3-CMeCMeCX ligand is linked by σ-bonds to the two hydrido-bridged Ru atoms and via an η^3-allyl linkage to the third Ru atom. The principal effect of changing X is to cause asymmetry in the (η^3-allyl)→Ru linkage such that the Ru–(X-bonded carbon) distance is 2.230 (9) Å for X = SEt, 2.251 (9) Å for X = Me, and 2.433 (5) Å for X = OMe; the literature value for X = NMe$_2$ is 2.689 (6) Å.

Introduction

Clusters of the type $(\mu$-H)$M_3(\mu_3$-η^3-RCCR′CR″)$(CO)_9$ are formed in a wide variety of reactions and have been the subjects of many studies. Crystal structures have been reported for $(\mu$-H)$Ru_3(\mu_3$-η^3-CMeCHCEt)$(CO)_9$ (R = 11.5%),[6] $(\mu$-H)$Ru_3(\mu_3$-η^3-$C_{12}H_{15})(CO)_9$ (R = 8.0%),[7] $(\mu$-H)$Os_3(\mu_3$-η^3-CHCHCOX)(CO)$_9$ (X = H (R = 6.0%), Me (R = 5.3%)),[8] $(\mu$-H)$Os_3(\mu_3$-η^3-CHCHCCHO)$(CO)_9$ (R = 6.6%),[9] and $(\mu$-H)$Ru_3(\mu_3$-η^3-CMeCHCNEt$_2)(CO)_9$ (R = 2.77%).[10] For all but $(\mu$-H)$Ru_3(\mu_3$-η^3-CMeCHCNEt$_2$)-$(CO)_9$, the cluster framework may be described as a nido polyhedron based upon a pentagonal bipyramid (I).

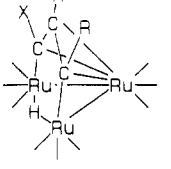

I

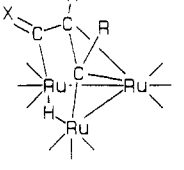

II

However, the structure of $(\mu$-H)$Ru_3(\mu_3$-η^3-CMeCHCNEt$_2)(CO)_9$ is distorted in a manner shown schematically in II. In previous papers we have described the synthesis and reactions of HRu_3(RCCRCX)$(CO)_9$ (X = OMe,[11] SEt;[12] R = H, alkyl, aryl). These clusters undergo unusual rearrangements involving cleavage of the C–X bond, while the derivative in which X = NR$_2$ does not. We were therefore interested in the structures adopted by these compounds, to determine whether the coordination of the C_3R_2X unit was affected by the nature of X. In this paper we report the crystal structures of $(\mu$-H)$Ru_3(\mu_3$-

(1) Structural Studies on Ruthenium Carbonyl Hydrides. 15. For recent contributions, see ref 2–5.
(2) Part 14: Janik, T. S.; Churchill, M. R.; Duggan, T. P.; Keister, J. B. *J. Organomet. Chem.* **1988**, *353*, 343.
(3) Part 13: Churchill, M. R.; Ziller, J. W.; Dalton, D. M.; Keister, J. B. *Organometallics* **1987**, *6*, 806.
(4) Part 12: Churchill, M. R.; Janik, T. S.; Duggan, T. P.; Keister, J. B. *Organometallics* **1987**, *6*, 799.
(5) Part 11: Churchill, M. R.; Duggan, T. P.; Keister, J. B.; Ziller, J. W. *Acta Crystallogr., Sect. C* **1987**, *C43*, 203.
(6) Evans, M.; Hursthouse, M.; Randall, E. W.; Rosenberg, E.; Milone, L.; Valle, M. *J. Chem. Soc., Chem. Commun.* **1972**, 545.
(7) Cox, A.; Woodward, P. J. *J. Chem. Soc. A* **1971**, 3599.
(8) Hanson, B. E.; Johnson, B. F. G.; Lewis, J.; Raithby, P. R. *J. Chem. Soc., Dalton Trans.* **1980**, 1852.
(9) Aime, S.; Tiripicchio, A.; Camellini, M. T.; Deeming, A. J. *Inorg. Chem.* **1981**, *20*, 2027.
(10) Aime, S.; Osella, D.; Deeming, A. J.; Arce, A. J.; Hursthouse, M. B.; Dawes, H. M. *J. Chem. Soc., Dalton Trans.* **1986**, 1459.
(11) Beanan, L. R.; Keister, J. B. *Organometallics* **1985**, *4*, 1713.
(12) Ziller, J. W.; Bower, D. K.; Dalton, D. M.; Keister, J. B.; Churchill, M. R. *Organometallics* **1989**, *8*, 492.

0276-7333/90/2309-0766$02.50/0

Table I. Crystallographic Data for the Three Cluster Compounds

(A) Unit Cell Parameters

	deriv		
	CMeCMeCMe	CMeCMeCOMe	CMeCMeCSEt
cryst syst	orthorhombic	monoclinic	monoclinic
space group	*Pnma* (No. 62)	$P2_1/n$ (No. 14)	$P2_1/n$ (No. 14)
a, Å	17.483 (11)	9.581 (2)	10.0275 (13)
b, Å	16.033 (9)	20.470 (3)	16.430 (3)
c, Å	7.105 (3)	10.7003 (15)	13.812 (2)
β, deg	90	106.400 (13)	107.976 (11)
V, Å^3	1992 (2)	2013.5 (5)	2164.4 (6)
Z	4	4	4
formula	$C_{15}H_{10}O_9Ru_3$	$C_{15}H_{10}O_{10}Ru_3$	$C_{16}H_{12}O_9Ru_3S$
mol wt	637.4	653.4	683.5
D(calcd), g cm^{-3}	2.13	2.16	2.10
μ, cm^{-1}	22.5	22.3	22.0
T, °C	23	23	23

(B) Measurement of Intensity Data

diffractometer: Syntex $P2_1$
radiation: Mo K$\bar{\alpha}$ ($\bar{\lambda}$ = 0.710 730 Å)
monochromator: pyrolytic graphite ($2\theta_{mono}$ = 12.2°), equatorial mode; assumed to be 50% perfect/50% ideally mosaic for polarizn cor
rflns measd: C_3Me_3 complex, 2989 for $+h,\pm k,+l$ and 2θ = 4.0–45.0°, merged to 1348 unique data with $|F_o| > 0$ (R_{int} = 1.54%); $C_3Me_2(OMe)$ complex, 3794 for $+h,+k,\pm l$ and 2θ = 4.5–50.0°, merged to 3356 unique data with $|F_o| > 0$ (R_{int} = 0.97%); $C_3Me_2(SEt)$ complex, 3037 for $+h,+k,\pm l$ and 2θ = 4.0–45.0°, merged to 2736 unique data with $|F_o| > 0$ (R_{int} = 1.36%)
scan conditions: coupled θ(crystal)–2θ(counter) scan at 4.0° min^{-1} in 2θ from $[2\theta(K\alpha_1) - 1.0]°$ to $[2\theta(K\alpha_2) + 1.0]°$; bkgds counted at each end of 2θ scan, each for $^1/_4$ of total scan time
std rflns: 3 approx mutually orthogonal rflns collected before each batch of 97 rflns; no signif fluctuations nor decay obsd
abs cor: empirical, by interpolation in 2θ and ϕ between normalized transmissn curves of close-to-axial ψ scans (not necessary for the $C_3Me_2(OMe)$ complex; see text)

η^3-CMeCMeCOMe)$(CO)_9$ and $(\mu$-H$)Ru_3(\mu_3$-η^3-CMeCMeCSEt$)(CO)_9$. Because previous structures of *undistorted* clusters of the class have been of limited precision, we have also determined the crystal structure of $(\mu$-H$)Ru_3(\mu_3$-η^3-CMeCMeCMe$)(CO)_9$. These are compared with the structure of $(\mu$-H$)Ru_3(\mu_3$-η^3-CMeCHCNEt$_2)(CO)_9$ to demonstrate the effect of C=X π bonding upon the structure adopted by the Ru_3C_3 core.

Experimental Section

Compounds. The compounds $(\mu$-H$)Ru_3(\mu_3$-η^3-CMeCMeMe$)(CO)_9$,[11] $(\mu$-H$)Ru_3(\mu_3$-η^3-CMeCMeCOMe$)(CO)_9$,[11] and $(\mu$-H$)Ru_3(\mu_3$-η^3-CMeCMeCSEt$)(CO)_9$[12] were prepared by using previously reported procedures. All compounds were recrystallized from methanol.

Collection of X-ray Diffraction Data for $(\mu$-H$)Ru_3(\mu_3$-η^3-CMeCMeCMe$)(CO)_9$. An orange crystal (0.27 mm × 0.27 mm × 0.22 mm) was inserted into a thin-walled capillary. It was then mounted in a eucentric goniometer and accurately centered on the Syntex $P2_1$ automated four-circle diffractometer at SUNY—Buffalo. Laue symmetry determination, crystal class, unit cell parameters, and the crystal's orientation matrix were carried out as described previously.[13] Intensity data (Mo Kα) were collected at room temperature (23 °C) with a coupled θ-(crystal)–2θ(counter) scan; details appear in Table I. All data were corrected for the effects of absorption and for Lorentz and polarization effects.

The crystal belongs to the orthorhombic system (diffraction symmetry D_{2h} or *mmm*). The systematic absences $0kl$ for $k + l = 2n + 1$ and $hk0$ for $h = 2n + 1$ are consistent with either the centrosymmetric space group *Pnma* (No. 62, D_{2h}^{16}) or the noncentrosymmetric space group $Pn2_1a$ (a nonstandard setting of $Pna2_1$, No. 33; C_{2v}^9). We therefore collected two octants of data (hkl and $h\bar{k}l$), so that the absolute configuration could be determined if the space group were to be the polar $Pn2_1a$. A total data set of 2989 reflections was collected. As a result of the later determination that the crystal belonged to the centrosymmetric space group *Pnma*, reflections were merged (R_{int} = 1.54% for 1256 pairs of reflections) to a unique data set of 1348 reflections with $|F_o| > 0$.

Solution and Refinement of the Crystal Structure for $(\mu$-H$)Ru_3(\mu_3$-η^3-CMeCMeCMe$)(CO)_9$. All crystallographic calculations were carried out with use of either the UCI-modified version of the UCLA Crystallographic Computing Package[14] or the SHELXTL PLUS program set.[15] The analytical scattering factors for neutral atoms were used throughout the analysis;[16a] both the real ($\Delta f'$) and the imaginary ($i\Delta f''$) components of anomalous dispersion[16b] were included in the calculations. The quantity minimized during least-squares analysis was $\sum w(|F_o| - |F_c|)^2$, where $w^{-1} = \sigma^2(|F_o|) + 0.0005|F_o|^2$.

The structure was solved by direct methods (SHELXTL PLUS) and difference-Fourier methods. All non-hydrogen atoms and the hydride ligand were located and their positional and thermal parameters refined. Hydrogen atoms of the methyl groups were located from a difference-Fourier map and were included in optimized tetrahedral positions with d(C–H) = 0.96 Å.[18] Refinement converged ($(\Delta/\sigma)_{max}$ = 0.017) with[17] R_F = 3.9%, R_{wF} = 4.3%, and GOF = 1.30 (NO:NV = 10.1:1) for all 1348 data; R_F = 2.7% and R_{wF} = 3.6% for those 1111 data with $|F_o| > 6\sigma(|F_o|)$. A final difference-Fourier map showed features only between –0.59 and +0.69 e/Å^3. Final atomic coordinates are collected in Table II.

Collection of X-ray Diffraction Data for $(\mu$-H$)Ru_3(\mu_3$-η^3-CMeCMeCOMe$)(CO)_9$. An orange crystal (0.15 mm × 0.2 mm × 0.4 mm) mounted along its extended direction was used for data collection; details are provided in Table I. A total of 3794 reflections was collected. All data were corrected for Lorentz and polarization effects but not for absorption since the profiles of ψ scans were essentially flat (±3%) and were in the same range as statistical fluctuations. The diffraction symmetry (C_{2h}; $2/m$) and the systematic absences ($h0l$ for $h + l = 2n + 1$ and $0k0$ for $k = 2n + 1$) uniquely define the centrosymmetric monoclinic space group $P2_1/n$, a nonstandard setting of $P2_1/c$ (No. 14, C_{2h}^5).

Solution and Refinement of the Crystal Structure for $(\mu$-H$)Ru_3(\mu_3$-η^3-CMeCMeCOMe$)(CO)_9$. The positions of the

(13) Churchill, M. R.; Lashewycz, R. A.; Rotella, F. J. *Inorg. Chem.* 1977, *16*, 265.

(14) UCLA Crystallographic Computing Package; University of California at Los Angeles, Los Angeles, CA, 1981. Strouse, C. personal communication.

(15) SHELXTL PLUS; Nicolet Instrument Corp.: Madison, WI, 1988.

(16) (a) *International Tables for X-Ray Crystallography*; Kynoch Press: Birmingham, England, 1974; Vol. 4, pp 99–101. (b) *Ibid.* pp 149–150.

(17) R_F (%) = $100(\sum||F_o| - |F_c||)/\sum|F_o|$. R_{wF} (%) = $100[\sum w(|F_o| - |F_c|)^2/\sum w|F_o|^2]^{1/2}$. GOF = $[\sum w(|F_o| - |F_c|)^2/(NO - NV)]^{1/2}$, where NO = number of observations and NV = number of variables.

(18) Churchill, M. R. *Inorg. Chem.* 1973, *12*, 1213.

Table II. Atomic Coordinates (×10⁴) and Equivalent Isotropic Displacement Parameters (Å² × 10³) for (μ-H)Ru₃(μ₃-η³-CMeCMeCMe)(CO)₉

	x	y	z	U(eq)[a]
Ru(1)	8245.8 (0.3)	7500	2611.0 (0.9)	38.8 (0.2)
Ru(2)	9163.6 (0.3)	6585.4 (0.3)	178.7 (0.7)	49.8 (0.2)
C(1)	7581 (4)	7500	-236 (11)	45 (3)
C(2)	7978 (3)	6730 (4)	46 (7)	46 (2)
C(3)	6728 (5)	7500	-693 (15)	68 (4)
C(4)	7482 (4)	5946 (4)	9 (9)	66 (2)
C(11)	9225 (5)	7500	3739 (14)	60 (3)
C(12)	7787 (3)	6650 (4)	4146 (9)	52 (2)
C(21)	10253 (4)	6566 (5)	739 (12)	80 (3)
C(22)	9239 (4)	6045 (5)	-2171 (11)	71 (3)
C(23)	9073 (4)	5558 (5)	1535 (11)	68 (3)
O(11)	9768 (4)	7500	4624 (9)	81 (3)
O(12)	7522 (3)	6151 (3)	5063 (7)	80 (2)
O(21)	10879 (3)	6518 (5)	1131 (13)	139 (4)
O(22)	9264 (3)	5687 (4)	-3570 (9)	108 (3)
O(23)	9041 (3)	4953 (3)	2366 (8)	97 (2)
H(1)	9198 (48)	7500	-1207 (163)	100 (34)
H(3A)	6661	7500	-2034	80
H(3B)	6494	7011	-167	80
H(4A)	7455	5737	-1256	80
H(4B)	7705	5529	810	80
H(4C)	6977	6076	446	80

[a] Equivalent isotropic U defined as one-third of the trace of the orthogonalized U_{ij} tensor.

three ruthenium atoms were determined from an automatic Patterson calculation (SHELXTL PLUS). The remaining non-hydrogen atoms and the bridging hydride ligand were located from difference-Fourier syntheses and were refined. Hydrogen atoms of the methyl groups were located from a difference-Fourier synthesis and were placed in optimized tetrahedral positions with d(C–H) = 0.96 Å.[18] Full-matrix least-squares refinement of $\sum w(|F_o| - |F_c|)^2$ (with $w^{-1} = \sigma^2(|F_o|) + 0.0008(|F_o|)^2$) led to convergence ($(\Delta/\sigma)_{max} = 0.001$) with $R_F = 3.5\%$, $R_{wF} = 4.2\%$, and GOF = 1.05 for 257 variables refined against all 3356 independent reflections (NO:NV = 13.1:1) with $|F_o| > 0$; $R_F = 2.4\%$ and $R_{wF} = 3.7\%$ for those 2739 data with $|F_o| > 6.0\ \sigma(|F_o|)$. A final difference-Fourier synthesis showed only features in the range -0.48 to +0.51 e/Å³. Final atomic coordinates are collected in Table III.

Collection of X-ray Diffraction Data for (μ-H)Ru₃(μ₃-η³-CMeCMeCSEt)(CO)₉. An orange crystal of dimensions 0.17 mm × 0.17 mm × 0.47 mm, mounted along its extended axis, was used for data collection. Details appear in Table I. A total of 3037 data was collected. All data were corrected for absorption and for Lorentz and polarization effects. The diffraction symmetry (C_{2h}; $2/m$) and systematic absences ($h0l$ for $h + l = 2n + 1$ and $0k0$ for $k = 2n + 1$) uniquely define the centrosymmetric monoclinic space group $P2_1/n$.

Solution and Refinement of the Crystal Structure of (μ-H)Ru₃(μ₃-η³-CMeCMeCSEt)(CO)₉. The positions of the three ruthenium atoms were determined from an automatic Patterson calculation (SHELXTL PLUS). The remaining non-hydrogen atoms were located from a series of difference-Fourier syntheses. The hydride atom was also located, as were the organic hydrogens, which were included in optimized positions. Refinement of this model converged with the unexpectedly high discrepancy index $R_F = 10.0\%$. A difference-Fourier synthesis now showed two prominent peaks approximately 1.0 Å from Ru(1) and from Ru(2) and 2.7 Å apart. We decided (after inspecting a total of three data sets!) that some form of crystallographic unpleasantness (disorder, twinning or, possibly, cocrystallization of an impurity) was causing this. Accordingly, we included these two features in the model (as atoms Ru(1′) and Ru(2′)) with their site occupancy factors (SOF's) coupled to those of Ru(1) and Ru(2). Full-matrix least-squares refinement of $\sum w(|F_o| - |F_c|)^2$ (with $w^{-1} = \sigma^2(|F_o|) + 0.0010(|F_o|)^2$) led to convergence ($(\Delta/\sigma)_{max} = 0.013$) with the drastically reduced residuals $R_F = 5.1\%$, $R_{wF} = 6.8\%$, and GOF = 1.61 for 284 variables refined against all 2736 independent reflections (NO:NV = 9.6:1) with $|F_o| > 0$; $R_F = 4.2\%$ and $R_{wF} = 6.4\%$ for those 2308 data with $|F_o| > 6.0\sigma(|F_o|)$.

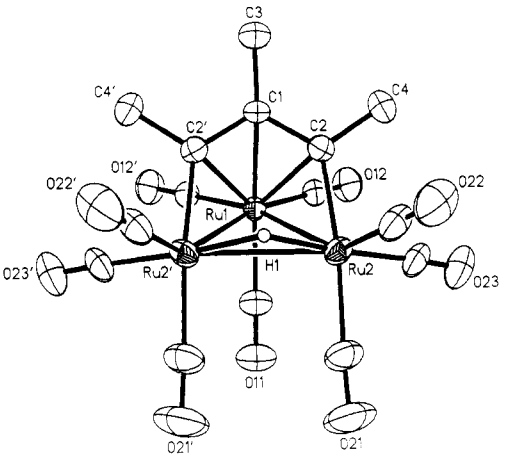

Figure 1. ORTEP-II diagram (30% probability ellipsoids) of (μ-H)Ru₃(μ₃-η³-CMeCMeCMe)(CO)₉ with the crystallographic mirror plane vertical.

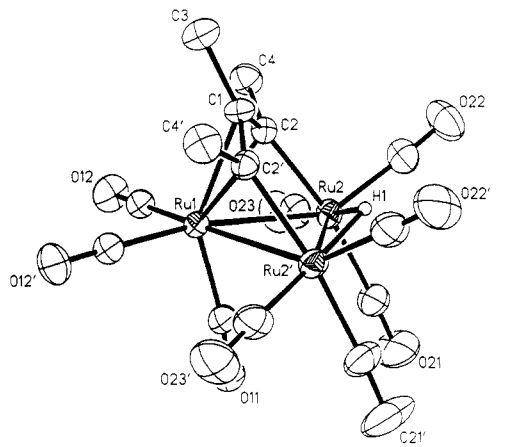

Figure 2. View of (μ-H)Ru₃(μ₃-η³-CMeCMeCMe)(CO)₉ showing the relative orientations of Ru₃, RuHRu, and CMeCMeCMe planes.

A final difference-Fourier map showed features in the range -0.74 to +1.41 e/Å³. The largest peak here is located ~0.8 Å from Ru(3) and is presumably associated with the disorder. Attempts to treat this as Ru(3′) (an atom of occupancy 0.1, similar to Ru(1′) and Ru(2′)) were unsuccessful, leading to substantially increased discrepancy indices. We assume that the resolution is not sufficient for us to treat Ru(3) and Ru(3′) as separate entities.

Final atomic coordinates are collected in Table IV.

Description of the Molecular Structures

All three species crystallize as molecular crystals with no abnormally close intermolecular contacts. Specific details for each compound appear below.

1. **(μ-H)Ru₃(μ₃-η³-CMeCMeCMe)(CO)₉.** This compound crystallizes in space group *Pnma*, and the molecule is bisected by a crystallographic mirror plane (at $y = {}^3/_4$) that passes through atoms H(3A), C(3), C(1), Ru(1), C(11), O(11), and H(1) (see Figures 1 and 2). Interatomic distances and angles are collected in Table V.

The hydrido-bridged Ru(2)–Ru(2′) distance is 2.933 (2) Å, some 0.156 Å longer than the nonbridged bonds Ru(1)–Ru(2) = Ru(1)–Ru(2′) = 2.777 (2) Å. The hydride ligand lies symmetrically between Ru(2) and Ru(2′) with Ru(2)–H(1) = Ru(2′)–H(1) = 1.77 (7) Å. The μ_3-η^3-CMeCMeCMe ligand is bonded symmetrically to the triruthenium cluster. The formal σ-bonds are Ru(2)–C(2) = Ru(2′)–C(2′) = 2.088 (6) Å, while the π-allyl linkage to Ru(1) is associated with terminal distances of Ru(1)–C(2) = Ru(1)–C(2′) = 2.251 (6) Å and a central distance of Ru(1)–C(1) = 2.333 (8) Å (i.e., 0.082 Å longer). Distances

Table III. Atomic Coordinates (×10⁴) and Equivalent Isotropic Displacement Coefficients (Å² × 10³) for (μ-H)Ru$_3$(μ_3-η^3-CMeCMeCOMe)(CO)$_9$

	x	y	z	U(eq)[a]
Ru(1)	0.2 (0.4)	1495.8 (0.2)	2409.8 (0.4)	40.4 (0.1)
Ru(2)	2912.9 (0.5)	1179.9 (0.2)	3237.9 (0.4)	44.6 (0.2)
Ru(3)	1955.9 (0.4)	1786.2 (0.2)	827.9 (0.3)	38.5 (0.1)
O(1)	3264 (6)	471 (2)	405 (4)	80 (2)
O(11)	−981 (7)	2923 (3)	2442 (5)	97 (2)
O(12)	−459 (6)	1347 (2)	5079 (4)	87 (2)
O(13)	−2965 (5)	982 (3)	918 (5)	97 (2)
O(21)	6139 (6)	1107 (4)	3446 (6)	132 (4)
O(22)	3361 (8)	548 (4)	5893 (5)	127 (3)
O(23)	2902 (5)	2559 (2)	4239 (4)	80 (2)
O(31)	1556 (6)	3255 (2)	1302 (5)	85 (2)
O(32)	5005 (5)	2143 (2)	757 (5)	78 (2)
O(33)	448 (6)	1833 (3)	−2073 (4)	93 (2)
C(1)	912 (6)	569 (2)	2494 (5)	49 (2)
C(2)	1889 (6)	355 (3)	1808 (5)	52 (2)
C(3)	2403 (6)	801 (2)	999 (5)	46 (2)
C(4)	320 (8)	37 (3)	3218 (7)	75 (3)
C(5)	2393 (9)	−352 (3)	1876 (7)	88 (4)
C(6)	3591 (7)	695 (3)	−712 (5)	59 (2)
C(11)	−577 (7)	2412 (3)	2421 (6)	62 (2)
C(12)	−1877 (7)	1203 (3)	1455 (6)	61 (2)
C(13)	−294 (7)	1392 (3)	4080 (6)	58 (2)
C(21)	4392 (8)	1128 (5)	3359 (6)	88 (3)
C(22)	3206 (8)	777 (3)	4897 (6)	74 (3)
C(23)	2815 (6)	2043 (3)	3804 (5)	56 (2)
C(31)	1682 (6)	2708 (3)	1131 (5)	57 (2)
C(32)	3868 (7)	2002 (3)	776 (5)	52 (2)
C(33)	1010 (7)	1832 (3)	−998 (6)	58 (2)
H(1)	226 (87)	1601 (40)	854 (75)	129 (29)
H(4A)	−558	−142	2650	80
H(4B)	1031	−304	3485	80
H(4C)	117	223	3971	80
H(5A)	1775	−592	1161	80
H(5B)	3377	−368	1828	80
H(5C)	2344	−542	2683	80
H(6A)	4215	386	−905	80
H(6B)	2708	743	−1405	80
H(6C)	4076	1109	−534	80

[a] Equivalent isotropic U defined as one-third of the trace of the orthogonalized U_{ij} tensor.

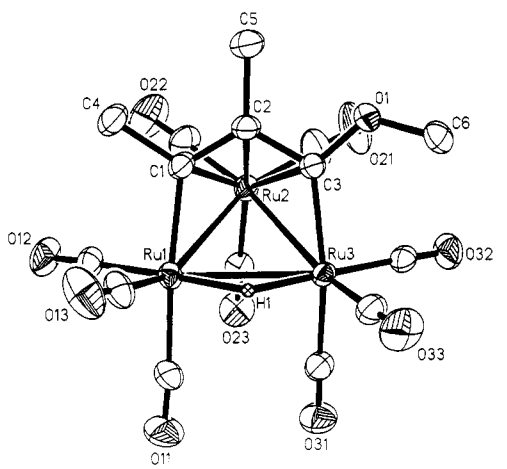

Figure 3. ORTEP-II (30% ellipsoids) view of (μ-H)Ru$_3$(μ_3-η^3-CMeCMeCOMe)(CO)$_9$ with the local pseudo mirror plane vertical.

within the allyl fragment are C(2)–C(1) = C(1)–C(2′) = 1.430 (7) Å with C–Me = 1.525 (11)–1.527 (9) Å. The Ru$_3$ system makes an angle of 39.4° with the Ru(2)–H(1)–Ru(2′) system and 60.2° with the least-squares plane through the C_3Me_3 system. The Ru(2)–H(1)–Ru(2′)/C_3Me_3 angle is 99.6°.

The Ru–C–O angles range from 171.5 (8) to 179.4 (6)° with Ru–CO = 1.886 (8)–1.945 (8) Å and C–O = 1.131 (8)–1.148 (10) Å. Of note is that the longest Ru–CO bonds,

Table IV. Atomic Coordinates (×10⁴) and Equivalent Isotropic Displacement Coefficients (Å² × 10⁴) for (μ-H)Ru$_3$(μ_3-η^3-CMeCMeCSEt)(CO)$_9$

	x	y	z	U(eq)[a]	SOF[b]
Ru(1)	1359.6 (0.9)	3302.4 (0.4)	274.5 (0.7)	364 (4)	0.90
Ru(2)	2145.4 (1.0)	1734.9 (0.4)	949.7 (0.7)	334 (3)	0.90
Ru(3)	3240.4 (0.7)	2377.0 (0.4)	−519.7 (0.5)	393 (3)	1.00
Ru(1′)	2175 (8)	3221 (4)	983 (6)	362 (28)	0.10
Ru(2′)	1432 (10)	1658 (4)	311 (8)	429 (33)	0.10
S(1)	2047 (4)	463 (2)	−1143 (3)	912 (17)	
C(1)	90 (10)	2270 (6)	−66 (7)	519 (36)	
C(2)	364 (9)	1552 (6)	−586 (6)	474 (34)	
C(3)	1730 (10)	1453 (5)	−697 (6)	463 (35)	
C(4)	−1309 (10)	2316 (7)	117 (9)	681 (45)	
C(5)	−720 (11)	883 (6)	−958 (9)	728 (47)	
C(6)	2342 (19)	548 (7)	−2311 (10)	1130 (82)	
C(7)	2354 (15)	−212 (7)	−2827 (10)	1009 (67)	
O(11)	3573 (10)	4675 (5)	1043 (9)	1082 (50)	
O(12)	411 (10)	3653 (6)	2129 (7)	1051 (47)	
O(13)	−834 (10)	4321 (5)	−1216 (7)	1029 (43)	
O(21)	4585 (9)	2726 (5)	2215 (6)	815 (34)	
O(22)	783 (10)	1488 (6)	2607 (8)	1178 (52)	
O(23)	3777 (9)	163 (5)	1486 (7)	895 (38)	
O(31)	5645 (8)	1151 (5)	−69 (7)	938 (39)	
O(32)	2768 (9)	2625 (5)	−2766 (6)	809 (37)	
O(33)	5586 (9)	3650 (5)	173 (7)	894 (38)	
C(11)	2773 (12)	4162 (6)	738 (10)	733 (53)	
C(12)	759 (12)	3517 (7)	1459 (10)	712 (51)	
C(13)	17 (12)	3946 (6)	−649 (8)	659 (45)	
C(21)	3634 (11)	2424 (6)	1664 (7)	526 (38)	
C(22)	1268 (12)	1576 (7)	1995 (8)	656 (46)	
C(23)	3134 (10)	730 (6)	1269 (8)	542 (39)	
C(31)	4718 (11)	1600 (6)	−248 (8)	596 (43)	
C(32)	2978 (9)	2526 (5)	−1938 (8)	478 (38)	
C(33)	4683 (11)	3204 (6)	−87 (8)	560 (41)	
H(1)	1780 (75)	3358 (40)	−694 (56)	334 (202)	
H(4A)	−1978	2575	−451	800	
H(4B)	−1623	1776	198	800	
H(4C)	−1218	2625	724	800	
H(5A)	−1303	996	−1639	800	
H(5B)	−259	369	−944	800	
H(5C)	−1289	861	−512	800	
H(6A)	3226	816	−2203	800	
H(6B)	1624	889	−2743	800	
H(7A)	2526	−122	−3465	800	
H(7B)	3082	−550	−2402	800	
H(7C)	1464	−477	−2946	800	

[a] Equivalent isotropic U defined as one-third of the trace of the orthogonalized U_{ij} tensor (U(iso) for H(1)). [b] The site occupation factor (SOF) is 1.0 for all non-ruthenium atoms.

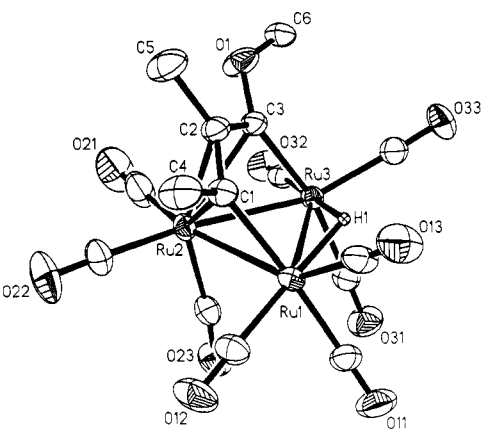

Figure 4. View of (μ-H)Ru$_3$(μ_3-η^3-CMeCMeCOMe)(CO)$_9$ showing the relative orientations of Ru$_3$, RuHRu, and CMeCMeCOMe planes.

Ru(2)–C(21) = Ru(2′)–C(21′) = 1.945 (8) Å, are those trans to the Ru–C σ-bonds (C(2)–Ru(2)–C(21) = C(2′)–Ru(2′)–C(21′) = 169.3 (3)°).

2. (μ-H)Ru$_3$(μ_3-η^3-CMeCMeCOMe)(CO)$_9$. The molecule is shown in Figures 3 and 4. Interatomic distances and angles are collected in Table VI. The hydrido-bridged Ru(1)–Ru(3) distance of 2.919 (1) Å is ~0.154 Å longer

Table V. Interatomic Distances (Å) and Angles (deg) with Esd's for $(\mu\text{-H})Ru_3(\mu_3\text{-}\eta^3\text{-CMeCMeCMe})(CO)_9$

Interatomic Distances			
Ru(1)-Ru(2)	2.777 (2)	Ru(2)-Ru(2′)	2.933 (2)
Ru(1)-C(1)	2.333 (8)	Ru(1)-C(2)	2.251 (6)
Ru(1)-C(11)	1.891 (9)	Ru(1)-C(12)	1.921 (6)
Ru(2)-H(1)	1.77 (7)	Ru(2)-C(2)	2.088 (6)
Ru(2)-C(21)	1.945 (8)	Ru(2)-C(22)	1.886 (8)
Ru(2)-C(23)	1.915 (8)	C(1)-C(2)	1.430 (7)
C(1)-C(3)	1.525 (11)	C(2)-C(4)	1.527 (9)
C(11)-O(11)	1.138 (11)	C(12)-O(12)	1.131 (8)
C(21)-O(21)	1.132 (9)	C(22)-O(22)	1.148 (10)
C(23)-O(23)	1.137 (9)		

Bond Angles			
Ru(2)-Ru(1)-C(1)	75.4 (2)	Ru(2)-Ru(1)-C(2)	47.7 (1)
C(1)-Ru(1)-C(2)	36.3 (2)	Ru(2)-Ru(1)-C(11)	75.0 (3)
C(1)-Ru(1)-C(11)	145.0 (4)	C(2)-Ru(1)-C(11)	122.1 (3)
Ru(2)-Ru(1)-C(12)	102.7 (2)	C(1)-Ru(1)-C(12)	106.5 (2)
C(2)-Ru(1)-C(12)	89.1 (2)	C(11)-Ru(1)-C(12)	97.9 (3)
Ru(2)-Ru(1)-Ru(2′)	63.7 (1)	C(2)-Ru(1)-Ru(2′)	84.6 (1)
C(12)-Ru(1)-Ru(2′)	165.8 (2)	C(2)-Ru(1)-C(2′)	66.5 (3)
C(12)-Ru(1)-C(2′)	139.6 (2)	C(12)-Ru(1)-C(12′)	90.3 (4)
Ru(1)-Ru(2)-C(2)	52.8 (2)	Ru(1)-Ru(2)-C(21)	116.5 (2)
C(2)-Ru(2)-C(21)	169.3 (3)	Ru(1)-Ru(2)-C(22)	146.5 (2)
C(2)-Ru(2)-C(22)	94.6 (3)	C(21)-Ru(2)-C(22)	96.0 (3)
Ru(1)-Ru(2)-C(23)	95.4 (2)	C(2)-Ru(2)-C(23)	92.1 (3)
C(21)-Ru(2)-C(23)	87.9 (3)	C(22)-Ru(2)-C(23)	93.2 (3)
Ru(1)-Ru(2)-H(1)	85.9 (29)	C(2)-Ru(2)-H(1)	85.2 (27)
C(21)-Ru(2)-H(1)	95.4 (27)	C(22)-Ru(2)-H(1)	83.4 (30)
C(23)-Ru(2)-H(1)	175.5 (33)	Ru(1)-Ru(2)-Ru(2′)	58.1 (1)
C(2)-Ru(2)-Ru(2′)	83.6 (2)	C(21)-Ru(2)-Ru(2′)	90.9 (2)
C(22)-Ru(2)-Ru(2′)	117.4 (2)	C(23)-Ru(2)-Ru(2′)	149.3 (2)
H(1)-Ru(2)-Ru(2′)	33.9 (30)	Ru(2)-H(1)-Ru(2′)	112 (6)
Ru(1)-C(1)-C(2)	68.7 (4)	Ru(1)-C(1)-C(3)	132.2 (6)
C(2)-C(1)-C(3)	120.3 (3)	C(2)-C(1)-C(2′)	119.3 (7)
Ru(1)-C(2)-Ru(2)	79.5 (2)	Ru(1)-C(2)-C(1)	75.0 (4)
Ru(2)-C(2)-C(1)	125.7 (4)	Ru(1)-C(2)-C(4)	125.7 (4)
Ru(2)-C(2)-C(4)	118.2 (4)	C(1)-C(2)-C(4)	115.7 (5)
Ru(1)-C(11)-O(11)	171.5 (8)	Ru(1)-C(12)-O(12)	179.4 (6)
Ru(2)-C(21)-O(21)	176.2 (8)	Ru(2)-C(22)-O(22)	176.8 (6)
Ru(2)-C(23)-O(23)	177.9 (7)		

than the average Ru–Ru distance of 2.765 Å (from Ru(1)–Ru(2) = 2.756 (1) Å and Ru(2)–Ru(3) = 2.774 (1) Å). Individual Ru–H distances are Ru(1)–H(1) = 1.75 (9) Å and Ru(3)–H(1) = 1.71 (9) Å (average 1.73 Å). Within the μ_3-η^3-CMeCMeCOMe ligand, the Ru–C σ-bonds are Ru(1)–C(1) = 2.081 (5) Å and Ru(3)–C(3) = 2.060 (5) Å; the first is close to the value observed in the C_3Me_3 complex, but the latter (associated with the OMe group) is slightly shorter (by 0.021 Å or $\sim 3.6\sigma$). The effect of the methoxy substituent on the π-allyl→Ru(2) linkage is more pronounced. The central Ru–C distance is Ru(2)–C(2) = 2.304 (5) Å. The terminal Ru–C distances are Ru(2)–C(1) = 2.238 (5) Å (at the Me end) and Ru(2)–C(3) = 2.433 (5) Å (at the OMe end); the difference of 0.196 Å clearly results from the electronic effects of the methoxy substituent, since the Ru(2)–C(1) and Ru(2)–C(2) distances are close to the equivalent bond lengths in the C_3Me_3 derivative whereas the Ru(3)–C(3) distance is not (2.433 (5) Å for the –OMe-bonded allylic carbon as opposed to a value of 2.251 (6) Å in the C_3Me_3 complex and 2.238 (5) Å for the other, Me-bonded, end of the π-allylic system within the CMeCMeCOMe complex).

The Ru_3 system makes an angle of 29.7° with the Ru(1)–H(1)–Ru(3) system and 52.4° with the C_3-allyl plane. The Ru(1)–H(1)–Ru(3)/C_3 angle is 81.9°.

Carbon–carbon distances within the allyl system are C(1)–C(2) = 1.412 (9) Å and C(2)–C(3) = 1.437 (8) Å; C–Me bond lengths are C(1)–C(4) = 1.535 (9) Å and C(2)–C(5) = 1.521 (8) Å, while the C–OMe system is defined by C(3)–O(1) = 1.356 (8) Å and O(1)–C(6) = 1.396 (8) Å.

The Ru–C–O angles range from 172.6 (5) to 178.7 (8)° with Ru–CO = 1.878 (7)–1.956 (7) Å and C–O = 1.117 (8)–1.148 (8) Å. Again, the two longest Ru–CO linkages are trans to the Ru–C σ-bonds. Thus, Ru(1)–C(11) = 1.956 (7) Å (associated with C(1)–Ru(1)–C(11) = 172.0 (2)°) and Ru(3)–C(31) = 1.944 (6) Å (associated with C(3)–Ru(3)–C(31) = 165.9 (2)°).

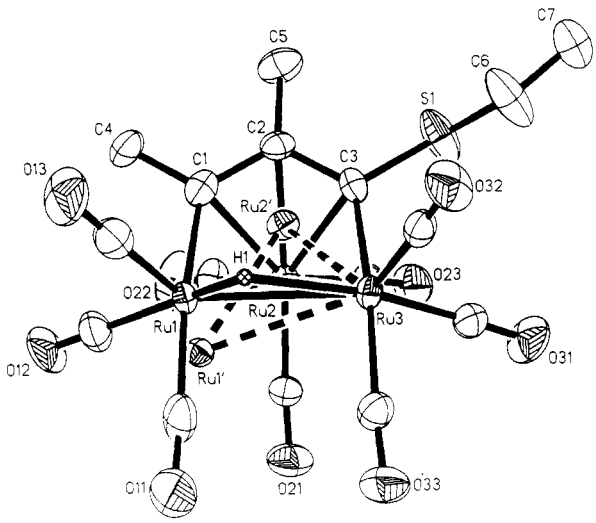

Figure 5. Structure of $(\mu\text{-H})Ru_3(\mu_3\text{-}\eta^3\text{-CMeCMeCSEt})(CO)_9$ with the local pseudo mirror plane vertical. Dashed lines denote the minor component of the disordered structure (ORTEP-II diagram, 30% probability ellipsoids).

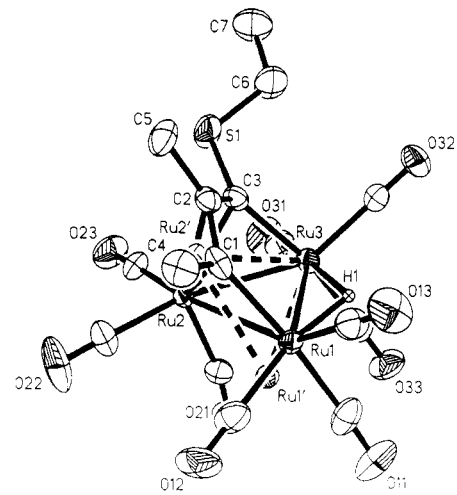

Figure 6. View of $(\mu\text{-H})Ru_3(\mu_3\text{-}^3\text{-CMeCMeCSEt})(CO)_9$ showing the relative orientations of Ru_3, RuHRu, and CMeCMeCSEt planes.

3. **$(\mu\text{-H})Ru_3(\mu_3\text{-}\eta^3\text{-CMeCMeCSEt})(CO)_9$.** The molecular structure is shown in Figures 5 and 6. Interatomic distances and angles are collected in Table VII.

As outlined in the Experimental Section (quod vide), this structure suffers from some form of crystallographic unpleasantness. The precise nature of this, on a molecular level, has not been fully elucidated. However, there appear to be two possible orientations of a Ru_3 triangle. The major orientation (90% occupancy) is based upon Ru(1), Ru(2), and Ru(3) and reveals the essential molecular geometry. The minor component (10% occupancy) is based upon Ru(1′), Ru(2′), and Ru(3) (or some location close to Ru(3)) and is not coplanar with the Ru(1)–Ru(2)–Ru(3) system but, rather, makes an angle of 42.2° with this plane. (The preparation and characterization of the compound is given in ref 12. There is no indication of an impurity in this sample, but the compound can isomerize to $Ru_3(\mu\text{-SEt})(\mu^3\text{-}\eta^3\text{-CCMeCHMe})(CO)_9$ in solution.)

This structural analysis is not as accurate as the first two because of the crystallographic problem. We have

Table VI. Interatomic Distances (Å) and Angles (deg) with Esd's for (μ-H)Ru_3(μ_3-η^3-CMeCMeCOMe)$(CO)_9$

Interatomic Distances

Ru(1)-Ru(2)	2.756 (1)	Ru(1)-Ru(3)	2.919 (1)	Ru(2)-C(3)	2.433 (5)	Ru(2)-C(21)	1.905 (8)
Ru(1)-H(1)	1.75 (9)	Ru(1)-C(1)	2.081 (5)	Ru(2)-C(22)	1.905 (6)	Ru(2)-C(23)	1.878 (7)
Ru(1)-C(11)	1.956 (7)	Ru(1)-C(12)	1.897 (6)	Ru(3)-H(1)	1.71 (9)	Ru(3)-C(3)	2.060 (5)
Ru(1)-C(13)	1.898 (6)	Ru(2)-Ru(3)	2.774 (1)	Ru(3)-C(31)	1.944 (6)	Ru(3)-C(32)	1.900 (7)
Ru(2)-C(1)	2.238 (5)	Ru(2)-C(2)	2.304 (5)	Ru(3)-C(33)	1.910 (5)		
C(1)-C(2)	1.412 (9)	C(1)-C(4)	1.535 (9)	C(3)-O(1)	1.356 (8)	C(6)-O(1)	1.396 (8)
C(2)-C(3)	1.437 (8)	C(2)-C(5)	1.521 (8)				
O(11)-C(11)	1.117 (8)	O(12)-C(13)	1.128 (8)	O(31)-C(31)	1.148 (8)	O(32)-C(32)	1.134 (8)
O(13)-C(12)	1.133 (7)	O(21)-C(21)	1.134 (10)	O(33)-C(33)	1.124 (7)		
O(22)-C(22)	1.135 (8)	O(23)-C(23)	1.148 (8)				

Interatomic Angles

Ru(2)-Ru(1)-Ru(3)	58.4 (1)	Ru(2)-Ru(1)-H(1)	87.1 (26)	Ru(1)-Ru(2)-C(22)	105.7 (2)	Ru(3)-Ru(2)-C(22)	169.4 (2)
Ru(3)-Ru(1)-H(1)	32.0 (26)	Ru(2)-Ru(1)-C(1)	52.9 (2)	C(1)-Ru(2)-C(22)	88.6 (3)	C(2)-Ru(2)-C(22)	103.0 (2)
Ru(3)-Ru(1)-C(1)	83.1 (2)	H(1)-Ru(1)-C(1)	89.4 (27)	C(3)-Ru(2)-C(22)	135.7 (2)	C(21)-Ru(2)-C(22)	91.9 (3)
Ru(2)-Ru(1)-C(11)	119.0 (2)	Ru(3)-Ru(1)-C(11)	92.1 (2)	Ru(1)-Ru(2)-C(23)	75.2 (2)	Ru(3)-Ru(2)-C(23)	81.1 (2)
H(1)-Ru(1)-C(11)	90.0 (27)	C(1)-Ru(1)-C(11)	172.0 (2)	C(1)-Ru(2)-C(23)	121.6 (2)	C(2)-Ru(2)-C(23)	148.5 (2)
Ru(2)-Ru(1)-C(12)	145.0 (2)	Ru(3)-Ru(1)-C(12)	114.7 (2)	C(3)-Ru(2)-C(23)	127.1 (2)	C(21)-Ru(2)-C(23)	99.9 (3)
H(1)-Ru(1)-C(12)	83.1 (26)	C(1)-Ru(1)-C(12)	93.3 (2)	C(22)-Ru(2)-C(23)	96.5 (3)	Ru(1)-Ru(3)-Ru(2)	57.8 (1)
C(11)-Ru(1)-C(12)	94.5 (3)	Ru(2)-Ru(1)-C(13)	94.4 (2)	Ru(1)-Ru(3)-H(1)	32.9 (26)	Ru(2)-Ru(3)-H(1)	87.3 (26)
Ru(3)-Ru(1)-C(13)	149.2 (2)	H(1)-Ru(1)-C(13)	178.5 (27)	Ru(1)-Ru(3)-C(3)	84.3 (2)	Ru(2)-Ru(3)-C(3)	58.2 (1)
C(1)-Ru(1)-C(13)	91.7 (2)	C(11)-Ru(1)-C(13)	89.1 (3)	H(1)-Ru(3)-C(3)	87.7 (27)	Ru(1)-Ru(3)-C(31)	87.8 (2)
C(12)-Ru(1)-C(13)	95.8 (3)	Ru(1)-Ru(2)-Ru(3)	63.7 (1)	Ru(2)-Ru(3)-C(31)	107.7 (2)	H(1)-Ru(3)-C(31)	92.0 (28)
Ru(1)-Ru(2)-C(1)	47.9 (1)	Ru(3)-Ru(2)-C(1)	83.9 (1)	C(3)-Ru(3)-C(31)	165.9 (2)	Ru(1)-Ru(3)-C(32)	147.8 (2)
Ru(1)-Ru(2)-C(2)	75.9 (1)	Ru(3)-Ru(2)-C(2)	75.1 (1)	Ru(2)-Ru(3)-C(32)	93.6 (2)	H(1)-Ru(3)-C(32)	179.1 (28)
C(1)-Ru(2)-C(2)	36.2 (2)	Ru(1)-Ru(2)-C(3)	81.6 (1)	C(3)-Ru(3)-C(32)	93.0 (2)	C(31)-Ru(3)-C(32)	87.5 (2)
Ru(3)-Ru(2)-C(3)	46.0 (1)	C(1)-Ru(2)-C(3)	63.8 (2)	Ru(1)-Ru(3)-C(33)	114.0 (2)	Ru(2)-Ru(3)-C(33)	155.5 (2)
C(2)-Ru(2)-C(3)	35.2 (2)	Ru(1)-Ru(2)-C(21)	162.1 (2)	H(1)-Ru(3)-C(33)	81.1 (26)	C(3)-Ru(3)-C(33)	99.5 (2)
Ru(3)-Ru(2)-C(21)	98.7 (2)	C(1)-Ru(2)-C(21)	138.1 (3)	C(31)-Ru(3)-C(33)	94.3 (2)	C(32)-Ru(3)-C(33)	98.1 (3)
C(2)-Ru(2)-C(21)	103.8 (3)	C(3)-Ru(2)-C(21)	88.1 (2)	Ru(1)-H(1)-Ru(3)	115.1 (40)		
Ru(1)-C(1)-Ru(2)	79.2 (2)	Ru(1)-C(1)-C(2)	126.3 (4)	Ru(2)-C(3)-Ru(3)	75.8 (2)	Ru(2)-C(3)-C(2)	67.5 (3)
Ru(2)-C(1)-C(2)	74.4 (3)	Ru(1)-C(1)-C(4)	117.3 (4)	Ru(3)-C(3)-C(2)	125.3 (4)	Ru(2)-C(3)-O(1)	129.9 (3)
Ru(2)-C(1)-C(4)	128.2 (4)	Ru(2)-C(2)-C(1)	69.4 (3)	Ru(3)-C(3)-O(1)	125.8 (4)		
Ru(2)-C(2)-C(3)	77.3 (3)	Ru(2)-C(2)-C(5)	126.6 (4)				
C(1)-C(2)-C(3)	120.4 (5)	C(2)-C(1)-C(4)	115.8 (5)	C(2)-C(3)-O(1)	108.9 (4)	C(3)-O(1)-C(6)	123.5 (5)
C(1)-C(2)-C(5)	121.2 (6)	C(3)-C(2)-C(5)	118.3 (6)				
Ru(1)-C(11)-O(11)	175.9 (7)	Ru(1)-C(12)-O(13)	174.7 (6)	Ru(3)-C(31)-O(31)	178.1 (6)	Ru(3)-C(32)-O(32)	178.5 (5)
Ru(1)-C(13)-O(12)	178.2 (5)	Ru(2)-C(21)-O(21)	178.7 (8)	Ru(3)-C(33)-O(33)	177.3 (5)		
Ru(2)-C(22)-O(22)	178.4 (7)	Ru(2)-C(23)-O(23)	172.6 (5)				

treated the light atoms of the major component as having 100% occupancy and have not located the nonmetallic atoms of the minor component. Keeping this potential systematic error in mind, we now consider the molecular geometry of (μ-H)Ru_3(μ_3-η^3-CMeCMeCSEt)$(CO)_9$.

Within the major component, the hydrido-bridged Ru(1)–Ru(3) distance is 2.889 (1) Å, some 0.107 Å longer than the average value of 2.782 Å for the nonbridged bonds Ru(1)–Ru(2) = 2.769 (1) Å and Ru(2)–Ru(3) = 2.795 (1) Å. The hydride ligand was located with uncertain reliability and is associated with the distances Ru(1)–H(1) = 1.52 (8) Å and Ru(3)–H(1) = 2.14 (7) Å.

The minor component of the Ru_3 system is associated with distances compatible with those of the major component (viz. Ru(1′)–Ru(2′) = 2.755 (10) Å, Ru(2′)–Ru(3) = 2.699 (11) Å, and Ru(1′)–Ru(3) = 2.956 (9) Å; a model with the last of these being hydrido bridged is possible).

The μ_3-η^3-CMeCMeCSEt ligand is associated with the Ru–C σ-bonds Ru(1)–C(1) = 2.086 (10) Å and Ru(3)–C(3) = 2.105 (9) Å; the first is similar to values observed in the C_3Me_3 ligand and at the Me end of the CMeCMeCOMe ligand, but the latter is marginally longer (but perhaps not so within statistical boundaries).

Within the π-allyl→Ru(2) linkage, the central atom is associated with the distance Ru(2)–C(2) = 2.332 (8) Å, while the terminal carbon atoms have Ru(2)–C(1) = 2.282 (9) Å and Ru(2)–C(3) = 2.230 (9) Å. The former is typical of the Me-substituted end of the μ_3-η^3-allyl system, while the latter (associated with –SEt substitution) is shorter than the value associated with either a –Me or an –OMe substituent.

The π-allyl system has the carbon–carbon bond lengths C(1)–C(2) = 1.451 (14) Å and C(2)–C(3) = 1.434 (14) Å. The C–Me distances are C(1)–C(4) = 1.502 (15) Å and C(2)–C(5) = 1.520 (13) Å, while the C–SEt system is defined by C(3)–S(1) = 1.801 (10) Å, S(1)–C(6) = 1.734 (16) Å, and C(6)–C(7) = 1.440 (18) Å.

The Ru(1)–Ru(2)–Ru(3)/C(1)–C(2)–C(3) interplanar angle is 61.8°.

The Ru–C–O systems are close to linear (167.6 (9)–178.9 (10)°), with Ru–CO = 1.870 (10)–1.964 (11) Å and C–O = 1.107 (18)–1.153 (13) Å. Once more, two of the longest Ru–CO bonds are trans to the σ-bonded carbon atoms of the allyl group. Thus, Ru(1)–C(11) = 1.964 (11) Å (associated with C(1)–Ru(1)–C(11) = 171.1 (4)°) and Ru(3)–C(33) = 1.940 (10) Å (associated with C(3)–Ru(3)–C(33) = 169.3 (4)°).

Discussion

The polyhedral skeletal electron pair theory and the isolobal analogy have proven useful in describing the structures of main-group and organotransition-metal complexes.[19] Viewed in this way, {η^5-(μ-H)$(Ru(CO)_3)_2$-$(CR)_3$}$Ru(CO)_3$ is isolobal with (η^5-C_5H_4X)FeL_2Y, both structures possessing eight skeletal electron pairs and six skeletal atoms and therefore considered as nido structures based upon the pentagonal bipyramid. The addition of

(19) (a) Wade, K. *Adv. Inorg. Chem. Radiochem.* **1976**, *18*, 1. (b) Mingos, D. M. P. *Nature (London), Phys. Sci.* **1972**, *236*, 99. (c) Evans, D. G.; Mingos, D. M. P. *Organometallics* **1983**, *2*, 435. (d) Mingos, D. M. P.; Johnston, R. L. *Struct. Bonding (Berlin)* **1987**, *68*, 29.

Table VII. Interatomic Distances (Å) and Angles (deg) with Esd's for $(\mu\text{-H})Ru_3(\mu_3\text{-}\eta^3\text{-CMeCMeCSEt})(CO)_9$

Interatomic Distances

Ru(1)-Ru(1′)	1.072 (7)	Ru(1)-Ru(2)	2.769 (1)	Ru(2)-Ru(3)	2.795 (1)	Ru(2)-C(1)	2.282 (9)
Ru(1)-Ru(2′)	2.704 (7)	Ru(1)-Ru(3)	2.889 (1)	Ru(2)-C(2)	2.332 (8)	Ru(2)-C(3)	2.230 (9)
Ru(1)-H(1)	1.52 (8)	Ru(1)-C(1)	2.086 (10)	Ru(2)-C(21)	1.891 (9)	Ru(2)-C(22)	1.926 (13)
Ru(1)-C(11)	1.964 (11)	Ru(1)-C(12)	1.942 (15)	Ru(2)-C(23)	1.906 (9)	Ru(2′)-Ru(3)	2.699 (11)
Ru(1)-C(13)	1.870 (10)	Ru(1′)-Ru(2)	2.442 (6)	Ru(3)-H(1)	2.14 (7)	Ru(3)-C(3)	2.105 (9)
Ru(1′)-Ru(2′)	2.755 (10)	Ru(1′)-Ru(3)	2.956 (9)	Ru(3)-C(31)	1.903 (10)	Ru(3)-C(32)	1.911 (11)
Ru(1′)-C(21)	1.973 (12)	Ru(2)-Ru(2′)	0.958 (9)	Ru(3)-C(33)	1.940 (10)		
S(1)-C(3)	1.801 (10)	S(1)-C(6)	1.734 (16)	C(2)-C(3)	1.434 (14)	C(2)-C(5)	1.520 (13)
C(1)-C(2)	1.451 (14)	C(1)-C(4)	1.502 (15)	C(6)-C(7)	1.440 (18)		
O(11)-C(11)	1.150 (14)	O(12)-C(12)	1.107 (18)	O(31)-C(31)	1.153 (13)	O(32)-C(32)	1.109 (14)
O(13)-C(13)	1.144 (13)	O(21)-C(21)	1.134 (12)	O(33)-C(33)	1.133 (13)		
O(22)-C(22)	1.107 (18)	O(23)-C(23)	1.120 (12)				

Interatomic Angles

Ru(2)-Ru(1)-Ru(3)	59.2 (1)	Ru(2′)-Ru(1)-Ru(3)	57.6 (2)	Ru(3)-Ru(1)-C(12)	145.4 (3)	H(1)-Ru(1)-C(12)	165.9 (25)
Ru(2)-Ru(1)-H(1)	103.0 (25)	Ru(3)-Ru(1)-H(1)	46.3 (25)	C(1)-Ru(1)-C(12)	90.6 (4)	C(11)-Ru(1)-C(12)	88.6 (5)
Ru(2)-Ru(1)-C(1)	53.9 (2)	Ru(3)-Ru(1)-C(1)	84.9 (3)	Ru(2)-Ru(1)-C(13)	145.7 (3)	Ru(3)-Ru(1)-C(13)	117.1 (4)
H(1)-Ru(1)-C(1)	99.6 (25)	Ru(2)-Ru(1)-C(11)	117.2 (3)	H(1)-Ru(1)-C(13)	72.7 (26)	C(1)-Ru(1)-C(13)	92.6 (4)
Ru(3)-Ru(1)-C(11)	90.7 (4)	H(1)-Ru(1)-C(11)	82.8 (25)	C(11)-Ru(1)-C(13)	96.3 (5)	C(12)-Ru(1)-C(13)	97.3 (5)
C(1)-Ru(1)-C(11)	171.1 (4)	Ru(2)-Ru(1)-C(12)	90.8 (3)	Ru(2)-Ru(1′)-Ru(3)	61.5 (2)	Ru(2′)-Ru(1′)-Ru(3)	56.3 (3)
Ru(1)-Ru(2)-Ru(3)	62.6 (1)	Ru(1′)-Ru(2)-Ru(3)	68.3 (2)	Ru(1)-Ru(2)-C(22)	103.3 (3)	Ru(3)-Ru(2)-C(22)	165.5 (3)
Ru(1)-Ru(2)-C(1)	47.6 (2)	Ru(3)-Ru(2)-C(1)	83.7 (3)	C(1)-Ru(2)-C(22)	88.7 (4)	C(2)-Ru(2)-C(22)	105.4 (4)
Ru(1)-Ru(2)-C(2)	75.8 (2)	Ru(3)-Ru(2)-C(2)	75.6 (3)	C(3)-Ru(2)-C(22)	138.7 (4)	C(21)-Ru(2)-C(22)	99.2 (5)
C(1)-Ru(2)-C(2)	36.6 (3)	Ru(1)-Ru(2)-C(3)	84.6 (2)	Ru(1)-Ru(2)-C(23)	163.1 (4)	Ru(3)-Ru(2)-C(23)	101.7 (4)
Ru(3)-Ru(2)-C(3)	47.9 (2)	C(1)-Ru(2)-C(3)	66.7 (3)	C(1)-Ru(2)-C(23)	141.5 (4)	C(2)-Ru(2)-C(23)	107.2 (4)
C(2)-Ru(2)-C(3)	36.6 (4)	Ru(1)-Ru(2)-C(21)	73.5 (3)	C(3)-Ru(2)-C(23)	88.6 (4)	C(21)-Ru(2)-C(23)	97.3 (4)
Ru(3)-Ru(2)-C(21)	74.3 (3)	C(1)-Ru(2)-C(21)	120.5 (4)	C(22)-Ru(2)-C(23)	92.0 (5)	Ru(1)-Ru(2′)-Ru(3)	64.7 (2)
C(2)-Ru(2)-C(21)	144.2 (4)	C(3)-Ru(2)-C(21)	121.7 (4)	Ru(1′)-Ru(2′)-Ru(3)	65.6 (3)		
Ru(1)-Ru(3)-Ru(2)	58.3 (1)	Ru(1)-Ru(3)-Ru(2′)	57.7 (2)	Ru(1)-Ru(3)-C(32)	115.0 (3)	Ru(2)-Ru(3)-C(32)	146.3 (3)
Ru(1′)-Ru(3)-Ru(2′)	58.1 (2)	Ru(1)-Ru(3)-H(1)	30.9 (22)	H(1)-Ru(3)-C(32)	85.2 (21)	C(3)-Ru(3)-C(32)	96.1 (4)
Ru(2)-Ru(3)-H(1)	87.5 (22)	Ru(1)-Ru(3)-C(3)	83.9 (3)	C(31)-Ru(3)-C(32)	98.1 (4)	Ru(1)-Ru(3)-C(33)	91.5 (3)
Ru(2)-Ru(3)-C(3)	51.8 (3)	H(1)-Ru(3)-C(3)	95.0 (19)	Ru(2)-Ru(3)-C(33)	117.6 (3)	H(1)-Ru(3)-C(33)	85.8 (18)
Ru(1)-Ru(3)-C(31)	146.9 (4)	Ru(2)-Ru(3)-C(31)	93.5 (4)	C(3)-Ru(3)-C(33)	169.3 (4)	C(31)-Ru(3)-C(33)	87.0 (4)
H(1)-Ru(3)-C(31)	172.3 (16)	C(3)-Ru(3)-C(31)	91.6 (4)	C(32)-Ru(3)-C(33)	94.6 (4)	Ru(1)-H(1)-Ru(3)	102.8 (34)
C(3)-S(1)-C(6)	110.1 (5)	Ru(1)-C(1)-Ru(2)	78.6 (3)	C(3)-C(2)-C(5)	119.3 (8)	Ru(2)-C(3)-S(1)	122.6 (4)
Ru(1)-C(1)-C(2)	125.2 (7)	Ru(2)-C(1)-C(2)	73.6 (5)	Ru(3)-C(3)-S(1)	119.6 (6)	Ru(2)-C(3)-C(2)	75.6 (5)
Ru(1)-C(1)-C(4)	117.3 (7)	Ru(2)-C(1)-C(4)	129.0 (7)	Ru(3)-C(3)-C(2)	125.6 (6)	S(1)-C(3)-C(2)	114.5 (7)
C(2)-C(1)-C(4)	117.0 (8)	Ru(2)-C(2)-C(1)	69.8 (4)	S(1)-C(6)-C(7)	114.8 (10)	Ru(1′)-C(21)-Ru(2)	78.4 (4)
Ru(2)-C(2)-C(3)	67.9 (4)	C(1)-C(2)-C(3)	118.6 (8)	Ru(1′)-C(21)-O(21)	112.1 (8)		
Ru(2)-C(2)-C(5)	131.9 (7)	C(1)-C(2)-C(5)	122.0 (9)				
Ru(1)-C(11)-O(11)	176.9 (13)	Ru(1)-C(12)-O(12)	178.7 (10)	Ru(3)-C(31)-O(31)	177.7 (9)	Ru(3)-C(32)-O(32)	176.9 (9)
Ru(1)-C(13)-O(13)	177.9 (10)	Ru(2)-C(21)-O(21)	167.6 (9)	Ru(3)-C(33)-O(33)	175.7 (9)		
Ru(2)-C(22)-O(22)	178.9 (10)	Ru(2)-C(23)-O(23)	176.2 (9)				

two more electrons to either of these structures is predicted to result in opening of the cage. If heteroatom substituents having free electron pairs are present, two electrons may be added to the skeletal electron count via π conjugation. The resulting structure might be described as an arachno structure based upon a dodecahedron if the C=X moiety is still to contribute one skeletal atom, but a description closer to the fact treats the C=X group as an edge-bridging ligand that contributes two electrons to the cage but does not contribute a skeletal atom.[19c] Then the structure will possess eight skeletal electron pairs but only five skeletal atoms and is described as an arachno structure based upon a pentagonal bipyramid. Qualitatively, these distortions may be explained by the increasing importance of resonance structure IV when the heteroatom is capable of

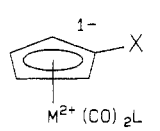

III

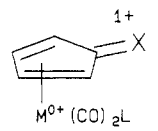

IV

π-donation into the five-membered ring, C_5H_4X or $(\mu\text{-H})(Ru(CO)_3)_2(CR)_2(CX)$. The structural distortions observed for $(\mu\text{-H})Ru_3(\mu_3\text{-}\eta^3\text{-CMeCMeCOMe})(CO)_9$ and $(\mu\text{-H})Ru_3(\mu_3\text{-}\eta^3\text{-CMeCHCNEt}_2)(CO)_9$ are consistent with this notion. For $(\mu\text{-H})Ru_3(\mu_3\text{-}\eta^3\text{-CMeCHCNEt}_2)(CO)_9$ only two

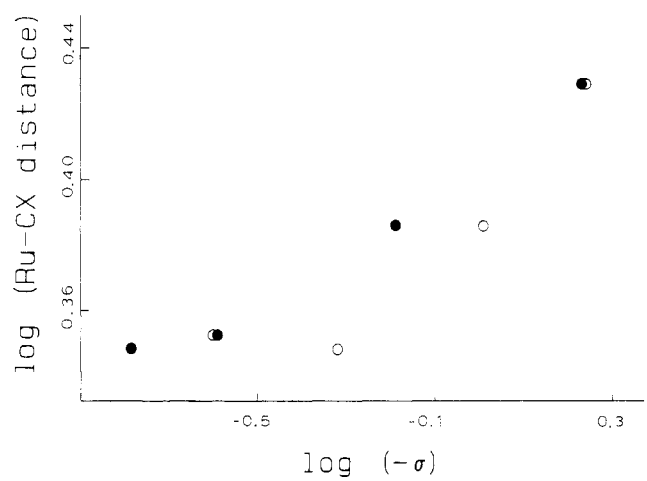

Figure 7. Correlation between log (Ru–CX distance) and log ($-\sigma$), where σ is the substituent constant σ_R^+ (○) or σ_p^+ (●).

carbon atoms of the $MeCCHCNMe_2$ unit are involved in the polyhedral skeleton; thus, the structure is properly described as an arachno structure, based upon seven vertices. The OMe group is a poorer π-donor than the NMe_2 group, and consequently, the structure adopted by $(\mu\text{-H})Ru_3(\mu_3\text{-}\eta^3\text{-CMeCMeCOMe})(CO)_9$ is intermediate between the nido and arachno structures. Accordingly,

Table VIII. Bond Distances for $HM_3(\mu_3$-η^3-XCCR'CR)$(CO)_9$ between the Metal Atom to Which the C_3 Unit Is η^3-Bonded and the 1- and 3-Carbons of the C_3 Unit

M	R	X	M–CR, Å	M–CX, Å	σ_R^+ [21]	σ_p^+ [20]	ref
Ru	Me	Et	2.37 (5)	2.34 (5)			6
Ru		c-$C_{12}H_{15}$	2.18 (3)	2.23 (3)			7
Os	H	OH	2.285 (43)	2.281 (34)			8
Os	H	OMe	2.246 (30)	2.405 (33)			8
Os	H	CHO	2.26 (2)	2.25 (2)			9
Ru	Me	NMe_2	2.248 (5)	2.689 (6)	−1.75	−1.7	10
Ru	Me	OMe	2.238 (5)	2.433 (5)	−1.02	−0.648	*a*
Ru	Me	SEt	2.282 (9)	2.230 (9)	−0.5	−0.164 (SMe)	*a*
Ru	Me	Me	2.251 (6)	2.251 (6)	−0.25	−0.256	*a*

[a] This work.

there is a monotonic relationship between the logarithm of the Ru–CX bond distance (proportional to log (Ru–CX bond energy)) and log ($-\sigma_p^+$), where the substituent parameter σ_p^+ is derived for substituents involved in π-conjugation with a reaction center in an electron-demanding transition state (Figure 7).[20] A less satisfactory correlation is found between the logarithm of the Ru–CX bond distance and log ($-\sigma_R^+$), where the substituent parameter σ_R^+ is a measure of the π-donor ability of X.[21] However, the value of σ_R^+ for the SEt substituent is not well-defined, and the precision of the Ru–CSEt bond length is not as high as for the others. Because of the few data points and the uncertainties in the bond distance for the SEt derivative and in the value of the substituent constant, it is pointless to attempt to quantitatively analyze the relationship. It is clear that the Ru–CX bond length generally increases as the expected π-donor ability of X increases (Table VIII).

A very similar nido–arachno distortion has been noted for the clusters $(\mu$-$H)_2Os_3(\mu_3$-η^2-XCCH$)(CO)_9$, although the authors chose to use a localized bonding model to rationalize these structures.[22] For X = OMe the structure may be described as a nido structure based upon an octahedron, while for X = NEt_2 lengthening of the Os–$CNEt_2$ bond generates a structure that may be described as arachno, based upon an octahedron.

Heteroatom substituents appear to induce similar distortions in the metal–carbon bond distances in cyclopentadienyl complexes.[23] The analogy between cyclopentadienyl and $(\mu$-H$)Ru_2(CRCRCX)^{2-}$ may prove to be useful in developing the chemistry of the class $(\mu$-H$)$-$Ru_3(\mu_3$-η^3-CRCRCX$)(CO)_9$. For example, ring slippage[24] may prove to be a mechanism for ligand substitution on the unique $Ru(CO)_3$ moiety and electrophilic aromatic substitution on the $(\mu$-H$)Ru_2(CRCRCX)^{2-}$ unit may be possible.

Acknowledgment. This work was supported in part by the National Science Foundation through Grant No. CHE8520276 (J.B.K.). J.B.K. also acknowledges a fellowship provided by the Alfred P. Sloan Foundation.

Supplementary Material Available: Tables of anisotropic thermal parameters (3 pages); listings of observed and calculated structure factor amplitudes (27 pages). Ordering information is given on any current masthead page.

(20) Swain, C. G.; Lupton, E. C., Jr. *J. Am. Chem. Soc.* **1968**, *90*, 4328; Gordon, A. J.; Ford, R. A. *The Chemist's Companion*; Wiley: New York, 1972; p 152.
(21) Ehrenson, S.; Brownlee, R. T. C.; Taft, R. W. *Prog. Phys. Org. Chem.* **1973**, *10*, 1.
(22) Deeming, A. J.; Kabir, S. E.; Nuel, D.; Powell, N. I. *Organometallics* **1989**, *8*, 717.
(23) Brun, P.; Vierling, J. G.; Le Borgne, G. *Organometallics* **1987**, *6*, 1032.
(24) Cheong, M.; Basolo, F. *Organometallics* **1988**, *7*, 2041.